



## Vacancy mechanism of oxygen diffusivity in bcc Fe: A first-principles study



S.L. Shang<sup>a,b,\*</sup>, H.Z. Fang<sup>a,b</sup>, J. Wang<sup>a,b,c</sup>, C.P. Guo<sup>a,b,d</sup>, Y. Wang<sup>a,b</sup>, P.D. Jablonski<sup>a,e</sup>, Y. Du<sup>c</sup>, Z.K. Liu<sup>a,b</sup>

<sup>a</sup> National Energy Technology Laboratory Regional University Alliance, U.S. Department of Energy, Pittsburgh, PA 15236, USA

<sup>b</sup> Department of Materials Science and Engineering, The Pennsylvania State University, University Park, PA 16802, USA

<sup>c</sup> State Key Laboratory of Powder Metallurgy, Central South University, Changsha, Hunan 410083, China

<sup>d</sup> Department of Materials Science and Engineering, University of Science and Technology Beijing, Beijing 100083, China

<sup>e</sup> National Energy Technology Laboratory, Department of Energy, Albany, OR 97321, USA

### ARTICLE INFO

#### Article history:

Received 13 December 2013

Accepted 2 February 2014

Available online 8 February 2014

#### Keywords:

- A. Iron
- B. Modeling studies
- C. Oxidation
- C. Internal oxidation

### ABSTRACT

Diffusivity of interstitial oxygen (O) in bcc iron (Fe) with and without the effect of vacancy has been investigated in terms of first-principles calculations within the framework of transition state theory. Examination of migration pathway and phonon results indicates that O in octahedral interstice is always energetically favorable (minimum energy) with and without vacancy. It is found that vacancy possesses an extremely high affinity for O in bcc Fe, increasing dramatically the energy barrier (~80%) for O migration, and in turn, making the predicted diffusion coefficient of O in bcc Fe in favorable accord with experiments.

© 2014 Elsevier Ltd. All rights reserved.

### 1. Introduction

Diffusion is a thermally activated process where a migrating atom passes through an energy barrier moving from a local energy minimum site to an adjacent vacant site. Diffusion determines a vast number of materials properties related to the transfer of mass such as the early stage of oxidation in Ni-based alloys [1], the corrosion of Al-based alloys under thin electrolyte layers [2], the marine immersion corrosion of mild steel [3], and the oxidation and corrosion of iron (Fe) associated with the present work. Despite technological importance and considerable experimental studies performed for diffusion of oxygen (O) in bcc Fe [4–10], little work regarding its fundamental mechanism has been studied compared to the interstitial diffusions of nitrogen (N) [11] and especially carbon (C) [12,13] in iron. Experimentally, diffusion coefficient of O in Fe alloys is typically estimated from internal-oxidation [10] owing to a very low solubility of O compared with other interstitial atoms of C and N in Fe and its alloys [8]. The activation energy for diffusion of O in bcc Fe is about  $1.0 \pm 0.1$  eV according to experiments performed by Takada et al. [8–10], Frank et al. [4,6], and Swisher and Turkdogan [5] (see details in Section 3).

However, first-principles predictions of activation energy for O diffusion in defect-free bcc Fe are only half and less (<0.54 eV) than experimental results regardless of the exchange correlation (X-C

functional as well as the consideration of charged species (the present results, see details in Section 3). The huge difference of diffusion activation energy between experiments and theoretic predictions suggests that some important facts are missed in first-principles calculations. On the other hand, both experiments and simulations indicate that the interstitial atoms such as C, H, O, and N have an exceptionally high affinity for vacancy (Va) in iron, and the migrating interstitial atoms are trapped by C-, H-, O-, and N-Va pairs [14–19]. For example, oxygen can serve as a Va-stabilizing agent [20]. Furthermore, Fu et al. [16] showed that the O-Va pairs in bcc Fe possess large negative binding energies (–1.45 and –0.6 eV for the first and the second nearest neighbors, respectively, see details and the definition of binding energy in Section 3), and enables the nucleation of a high density of stable nanoclusters in Fe-based alloys processed by mechanical alloying.

The present work is motivated by the dearth of first-principles study of O diffusion in bcc Fe, and in particular, the huge difference of activation energy between experiments and predictions regarding the diffusion of O in defect-free bcc Fe. Recently it has been demonstrated that the quantitative diffusion properties as a function of temperature including jump rates and migration barriers can be predicted in solid phases in terms of first-principles calculations within the framework of transition state theory [21–28]. In the present work, diffusion of O in bcc Fe with and without the effect of vacancy is studied through first-principles calculations based on the reaction rate theory of Eyring [29] as well as the transition state theory of Vineyard [30]. The climbing image nudged

\* Corresponding author. Tel.: +1 814 863 9957.

E-mail address: [sus26@psu.edu](mailto:sus26@psu.edu) (S.L. Shang).

elastic band (CINEB) method [31] is used to search the transition state (i.e., the saddle point). The phonon calculations in terms of the supercell method [32,33] as well as the Debye model [34] are used to predict thermodynamic properties at finite temperatures for various states during diffusion. Details of these computational methods are given in Section 2. We find a dramatic effect of vacancy on the predicted diffusion properties of O in bcc Fe, and the deeply trapped O by Va is found owing to an increased bending deformation resistance of O in terms of differential charge density and phonon force constants (see Section 3). Finally, in Section 4 the conclusions of the present work are given.

## 2. Computational methods

### 2.1. Interstitial diffusion coefficient and first-principles thermodynamics

Diffusion of interstitial solute atoms in solid solutions can be described as random jumps between interstitial positions. According to Wert and Zener [35], theoretical diffusion coefficient  $D$  of an interstitial atom in a cubic lattice can be described by,

$$D = n\beta d^2 \Gamma \quad (1)$$

where  $n$  is the number of the nearest neighbor (NN) interstitial positions,  $2\beta$  the probability when an interstitial atom jumps into a new interstitial position, and  $d$  the projected length onto the diffusion direction. For the present octahedral interstitial diffusion in bcc lattice,  $n = 4$ ,  $\beta = 1/6$ , and  $d = a/2$  with  $a$  being the lattice parameter [35]. Note that these values also hold when a NN vacancy is introduced to an interstitial atom. Fig. 1 illustrates a  $1 \times 1 \times 1$  supercell of bcc lattice (atoms located at Wyckoff site 2a of space group  $Im\bar{3}m$ ) together with its octahedral interstitial positions (Wyckoff site 6b) and tetrahedral interstitial positions (Wyckoff site 12d). Symbol  $\Gamma$  in Eq. (1) represents the jump rate [27,28,35],

$$\Gamma = \frac{k_B T}{h} \frac{Z_{TS}}{Z_{IS}} \exp\left(-\frac{\Delta E}{k_B T}\right) \quad (2)$$

where  $Z_{TS}$  and  $Z_{IS}$  are the partition functions of the transition state (TS) and the ground state of initial state (IS), respectively,  $k_B$  the Boltzman's constant,  $T$  the temperature, and  $h$  the Planck's constant.  $\Delta E$  is the energy difference between the TS (i.e., saddle point) and the IS, corresponding to the migration energy barrier. At high temperatures, the jump rate of Eq. (2) reduces to the result of Vineyard [30],

$$\Gamma = \frac{\prod_{i=1}^{3N-3} \nu_i^{IS}}{\prod_{i=1}^{3N-4} \nu_i^{TS}} \exp\left(-\frac{\Delta E}{k_B T}\right) \quad (3)$$

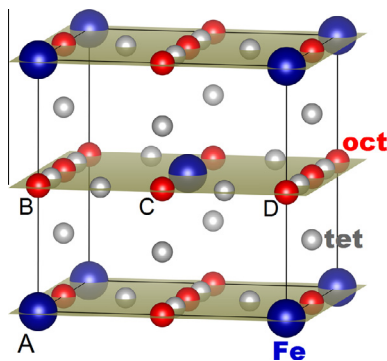


**Fig. 1.**  $1 \times 1 \times 1$  Supercell of bcc lattice with Fe metals located at Wyckoff site 2a of space group  $Im\bar{3}m$ , together with the octahedral interstitial positions (oct, Wyckoff site 6b) and tetrahedral interstitial positions (tet, Wyckoff site 12d). As an example with one vacancy (Va) at position A, the oct sites B, C, and D are its first, second, and third nearest neighbors (1NN, 2NN, and 3NN), respectively.

where  $\nu_i$  is the real normal modes of vibration, and  $N$  the total vibrating atoms. There are  $(3N - 3)$  non-zero optical modes for the IS and the TS at zone center, and one imaginary optical mode should be removed for the TS. In the present work, the products of  $\Pi \nu_i$  at different volumes are combined with the volume vs. temperature relationship obtained from the first-principles quasiharmonic approach (see Eq. (6)), therefore,  $\Pi \nu_i$  is expressed as a function of temperature herein. This volume-temperature transfer refers to the quasistatic approach, which has been used previously to predict the temperature dependences of elasticity [36,37], ideal shear strength [38], and stacking fault energy [39]. At low temperatures, the jump rate of Eq. (2) reduces to the reaction rate theory found by Eyring [29],

$$\Gamma = \frac{k_B T}{h} \exp\left(-\frac{\Delta E + \Delta E_{ZPE}}{k_B T}\right) \quad (4)$$

Here,  $\Delta E_{ZPE}$  is the zero-point vibrational energy difference between the TS and the IS. In practice and also in the present work,  $\Delta E$  in Eq. (3) and  $(\Delta E + \Delta E_{ZPE})$  in Eq. (4) are replaced by the temperature dependent Gibbs energy difference  $\Delta G$  (or Helmholtz energy difference  $\Delta F$  in the case of zero external pressure) between the TS and the IS estimated using the first-principles quasiharmonic approach of Eq. (6). The application of  $\Delta G$  or  $\Delta F$  is an efficient and accurate way to predict jump rate at finite temperatures [24,27], even without phonon calculations (see below). It is worth mentioning that it is a common practice to represent the diffusion coefficient (e.g., obtained by Eq. (1)) according to Arrhenius equation,

$$D = D_0 \exp\left(\frac{-Q}{k_B T}\right) \quad (5)$$

where  $D_0$  is a pre-exponential factor, and  $Q$  the activation energy (enthalpy) for diffusion.

Within the quasiharmonic approach, first-principles calculations based on the density functional theory (DFT) yield quantitative Helmholtz energy  $F$  for a given structure under volume  $V$  and temperature  $T$ , which can be approximately separated into [34,40,41],

$$F(V, T) = E(V) + F_{vib}(V, T) + F_{el}(V, T) \quad (6)$$

where  $E$  is the static total energy at 0 K without the zero-point vibrational energy, which is determined herein by fitting the first-principles energy vs. volume data points according to a four-parameter Birch–Murnaghan equation of state (EOS) with its linear form given by [34],

$$E(V) = a + bV^{-2/3} + cV^{-4/3} + dV^{-2} \quad (7)$$

where  $a$ ,  $b$ ,  $c$ , and  $d$  are fitting parameters. The equilibrium properties estimated from this EOS include the volume ( $V_0$ ), energy ( $E_0$ ), bulk modulus ( $B_0$ ) and its pressure derivative ( $B'_0$ ). In the present work, six to eight energy-volume data points are used for EOS fitting for the structure of interest. The second term  $F_{vib}(V, T)$  and the third term  $F_{el}(V, T)$  in Eq. (6) are related to contributions at finite temperatures.  $F_{el}$  is particularly important for metals due to the non-zero electronic density at the Fermi level, which can be estimated from the electronic densities of state at different volumes [34,40,41].  $F_{vib}$  is the vibrational contribution to  $F(V, T)$ , which can be calculated from (i) the Debye model via the equilibrium properties estimated from Eq. (7) for the sake of simplicity and (ii) the phonon density of state via first-principles phonon calculations. In the present work, both the Debye–Grüneisen model and the phonon method are adopted to calculate  $F_{vib}$  with the detailed methodologies given in [34].

Regarding the diffusion of oxygen in vacancy-included bcc Fe, only one major jump of oxygen with the maximum energy barrier is adopted in the present work, this jump determines mainly the

Download English Version:

<https://daneshyari.com/en/article/1468875>

Download Persian Version:

<https://daneshyari.com/article/1468875>

[Daneshyari.com](https://daneshyari.com)